Supplementary Material

Mono- and Biallelic Inactivation of Huntingtin Gene in Patient-Specific Induced Pluripotent Stem Cells Reveal HTT Roles in Striatal Development and Neuronal Functions

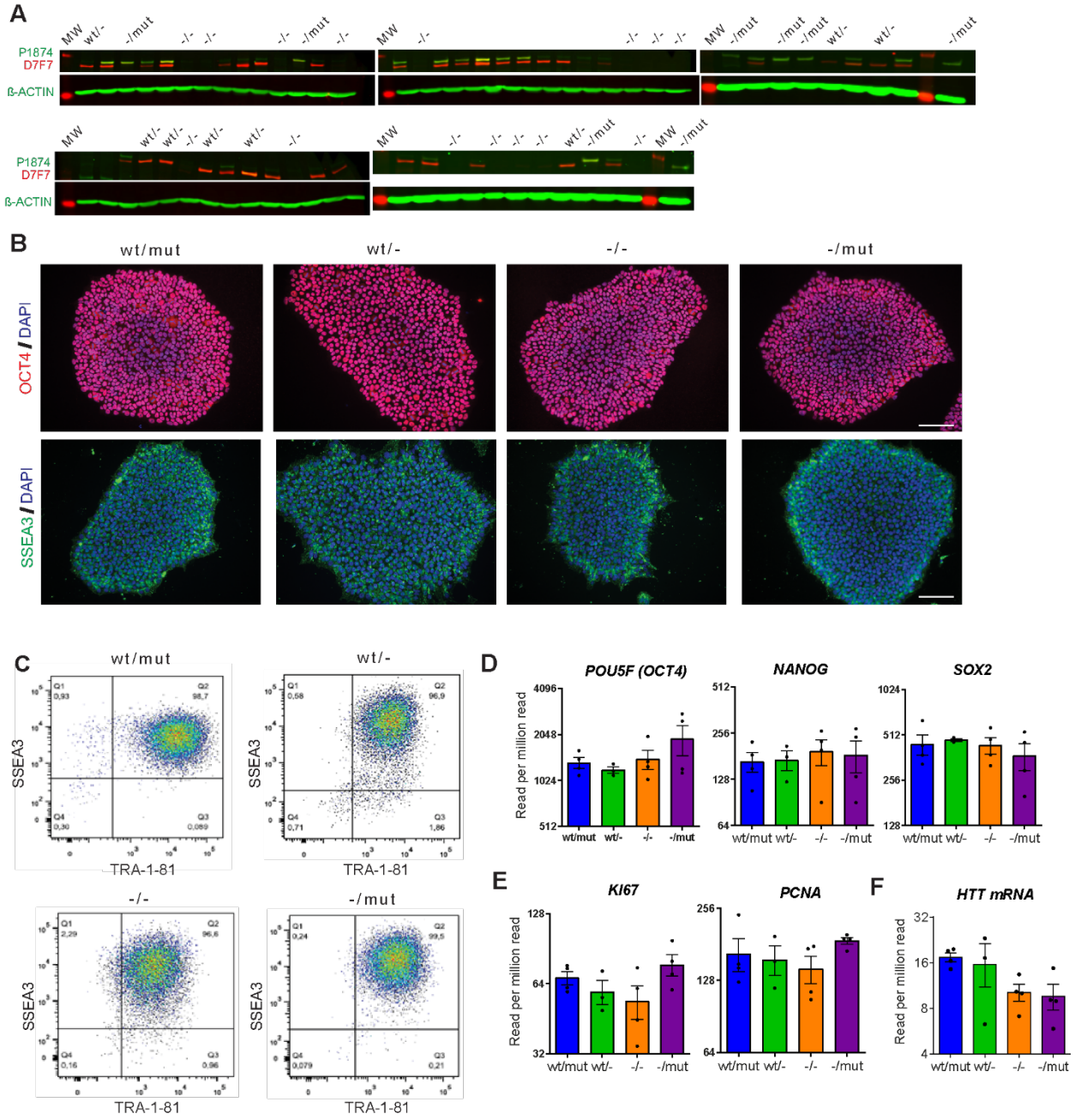

Supplementary Figure 1. Generation and validation of isogenic clones of 109Q-iPSC with monoallelic or biallelic *HTT* inactivation. A) Screening by western blot using two antibodies targeting HTT (D7F7) or mutant HTT (P1874) of 56 clones for monoallelic or biallelic

inactivation: 16 knockout homozygous clones (HTT-/-: clone 16 yy zz); 8 clones HTTwt/-; 8 clones HTT-/mut. B) Example of immunofluorescence for two pluripotency markers (Oct4, red and SSEA3, green) and DNA staining (DAPI, blue) (scale bar: 100 μm). C) Flow cytometry quantification of two membrane bound markers of pluripotency (SSEA3 and TRA1-81). D-F) RNAseq expression data for genes related to pluripotency (D) proliferation (E) and for HTT (NM_002111) (F) expressed in read per million reads. Expression of those genes are stable across geneotypes (n=4-3 clones/genotype, individual data point, mean and SEM are shown).

	WT Allele			Mutant Allele		
	indels in bp	Frameshift	Premature STOP	indels in bp	Frameshift	Premature STOP
wt/mut Parental	-	-	NO	-	-	NO
wt/- clone 1	-	-	NO	-32	+1	**YES**
wt/- clone 2	-	-	NO	-4	+2	**YES**
-/- clone 1	+1	+1	**YES**	+1	+1	**YES**
-/- clone 2	+1	+1	**YES**	+1	+1	**YES**
-/mut clone 1	-10	+2	**YES**	-	-	NO
-/mut clone 2	+1	+1	**YES**	-18	+0	NO

Supplementary Figure 2. Sequencing results of *HTT-gene* edition in iPSC isogenic clones by TIDE analysis.

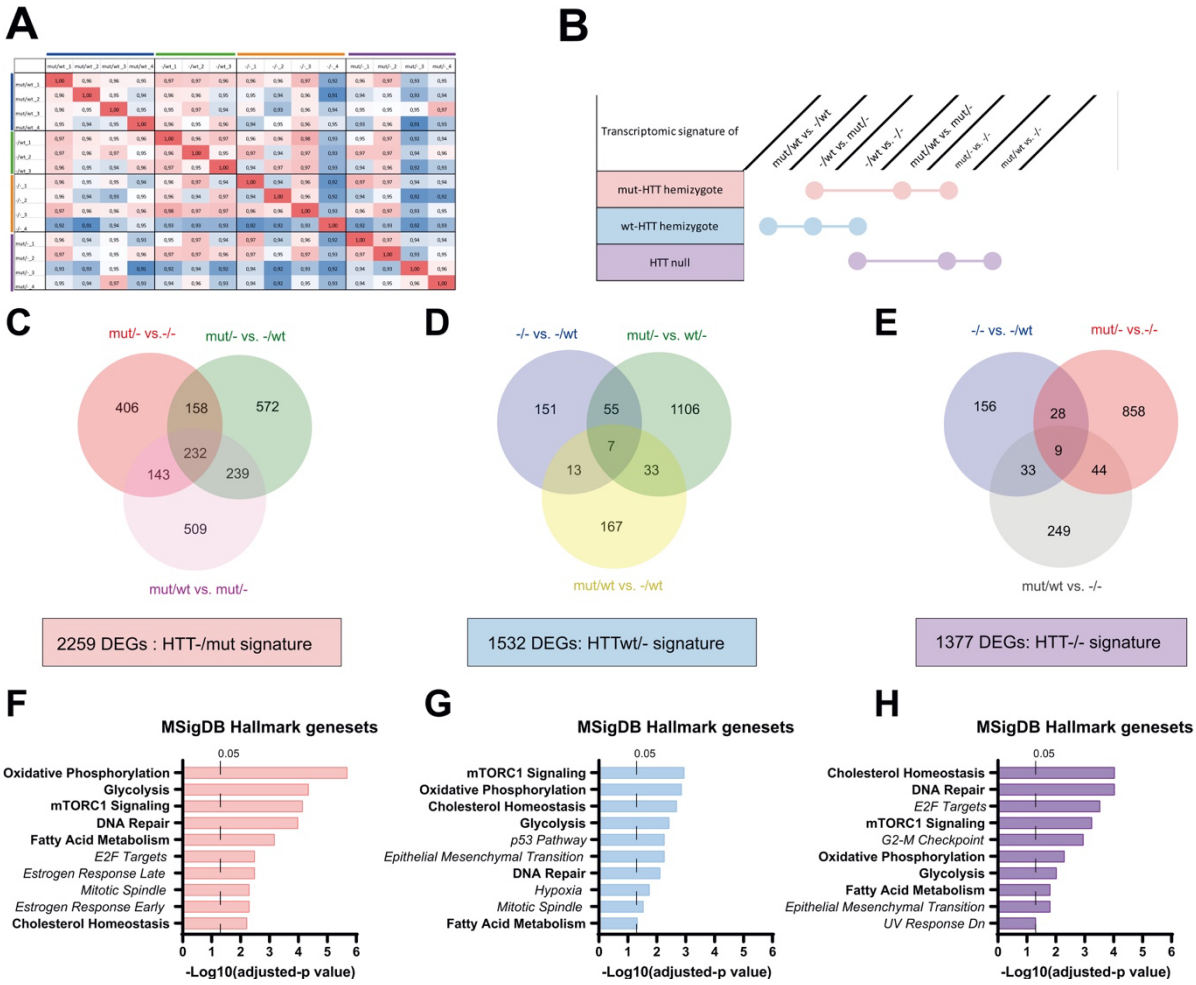

Supplementary Figure 3. Transcriptome analysis of isogenic HTTwt/mut, HTTwt/-; HTT-/mut and HTT -/- iPSC cells reveal shared signature of HTT loss and mutation. A) The correlation matrix of each samples shows no clustering by genotype of the different isogenic clones. B) Assignment table by category of pairwise comparisons used to profile three transcriptomic signatures (mutant-HTT gain of function; wild-type-HTT gain of function and HTT knock-out (i.e., wild-type and/or mutant-HTT loss of function). Venn diagram and MSigDB Hallmark genset enrichment scores of the 528 DEGs for the transcriptomic signature of mut-HTT gain of function (C), the 134 DEGs for the transcriptomic signature of wt-HTT loss of function (D) and the 114 DEGs for the transcriptomic signatures of total HTT knock-out (E). F-H) Venn diagram of TOP25 MSigDB Hallmark gensets of pairwise comparison by signature. (n=3-4 edited clones by genotypes)

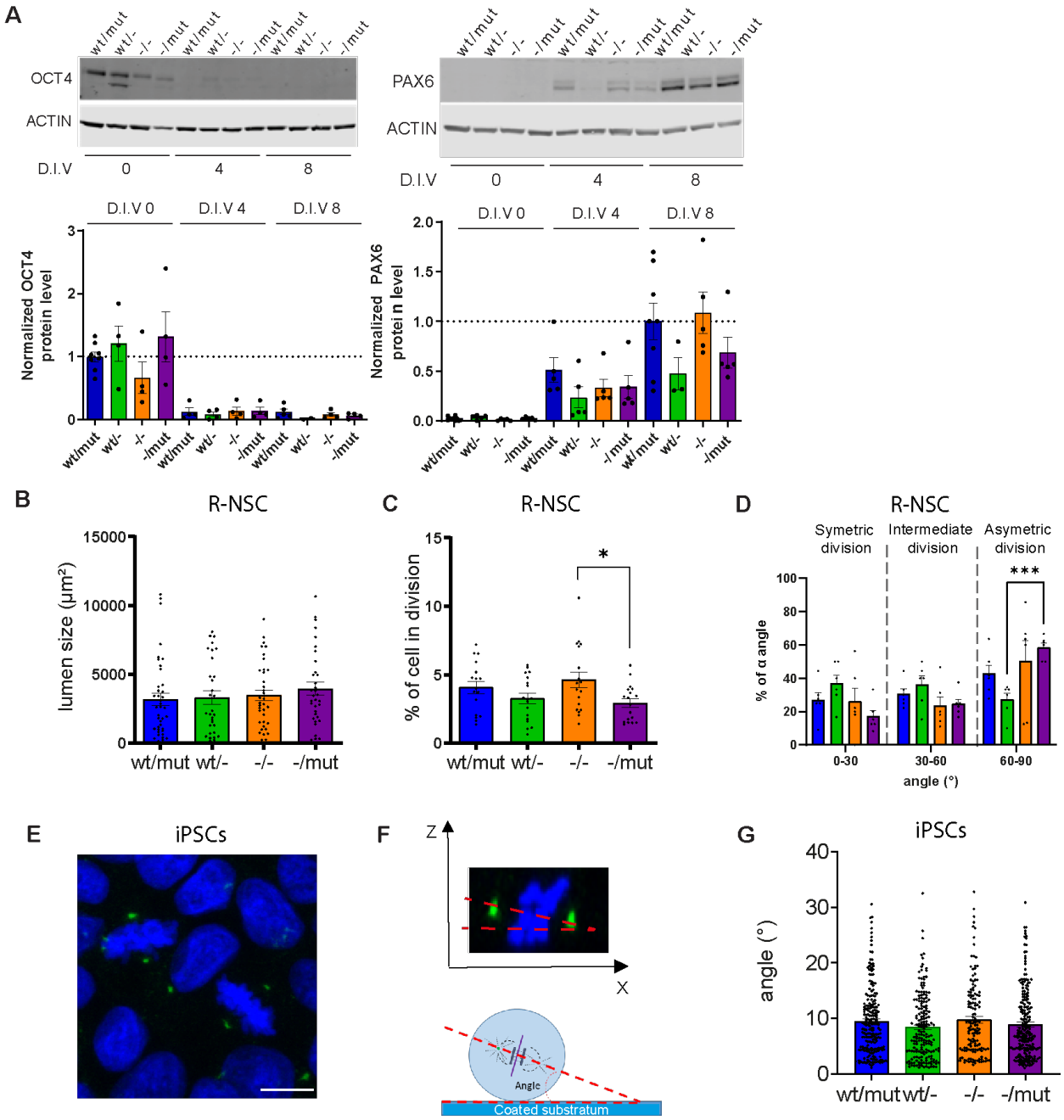

Supplementary Figure 4. Phenotypes of iPS and early neural cells derived from isogenic clones. Dual SMAD inhibition can trigger neural induction off all the isogenic clones. A) Representative western blot and quantification illustrating the loss of pluripotency (left) and the neural induction (right) during the first 8 days of differentiation. OCT4 (POU5F1), a pluripotency marker is equally downregulated at DIV4 independently of the genotype of the iPS while PAX6, an early neural marker in human embryo, is equally upregulated by DIV4 in all cultures (n=2 clones per genotype; Individual data point, mean and SEM are shown). B) Quantification of lumen size. Individual data points, mean and SEM are shown (n>30 rosette/ clones). C) Percentage of cells in division in all isogenic clones is higher in HTT-/- iPS colonies than in HTT-/mut colonies, each data point corresponds to the percentage of cells in division in one picture, for each isogenic clones: 6 pictures by well; two well by experiment; three independent experiments were analyzed. Individual data

points, mean and SEM are shown. *p<0.05, one-way ANOVA test with Tukey's multiple comparison post-test. (D) Quantification of the frequency of each type of cell's division in R-NSCs. Percentage of cells with asymmetric division is higher in R-NSC derived from HTT-/mut clones compared to HTTwt/- clones. Individual data points, mean and SEM are shown. ***p<0.001, one-way ANOVA test with Tukey's multiple comparison post-test. E) Representative immunostaining of pericentrin (green) to identified centrosomes of cells in division and DNA staining (DAPI, blue) in undifferentiated iPSCs (scale bar: 10 μm). F) Z-stack immunostaining and schema to illustrate the measurement of the spindle angle α between the pole-pole axis (the axis of the metaphase spindle) and the substratum plane in undifferentiated cells. G) Quantification of α angles relative to the coated substratum. Individual data point, mean and SEM are shown (n=140-219) from three independent experiment.

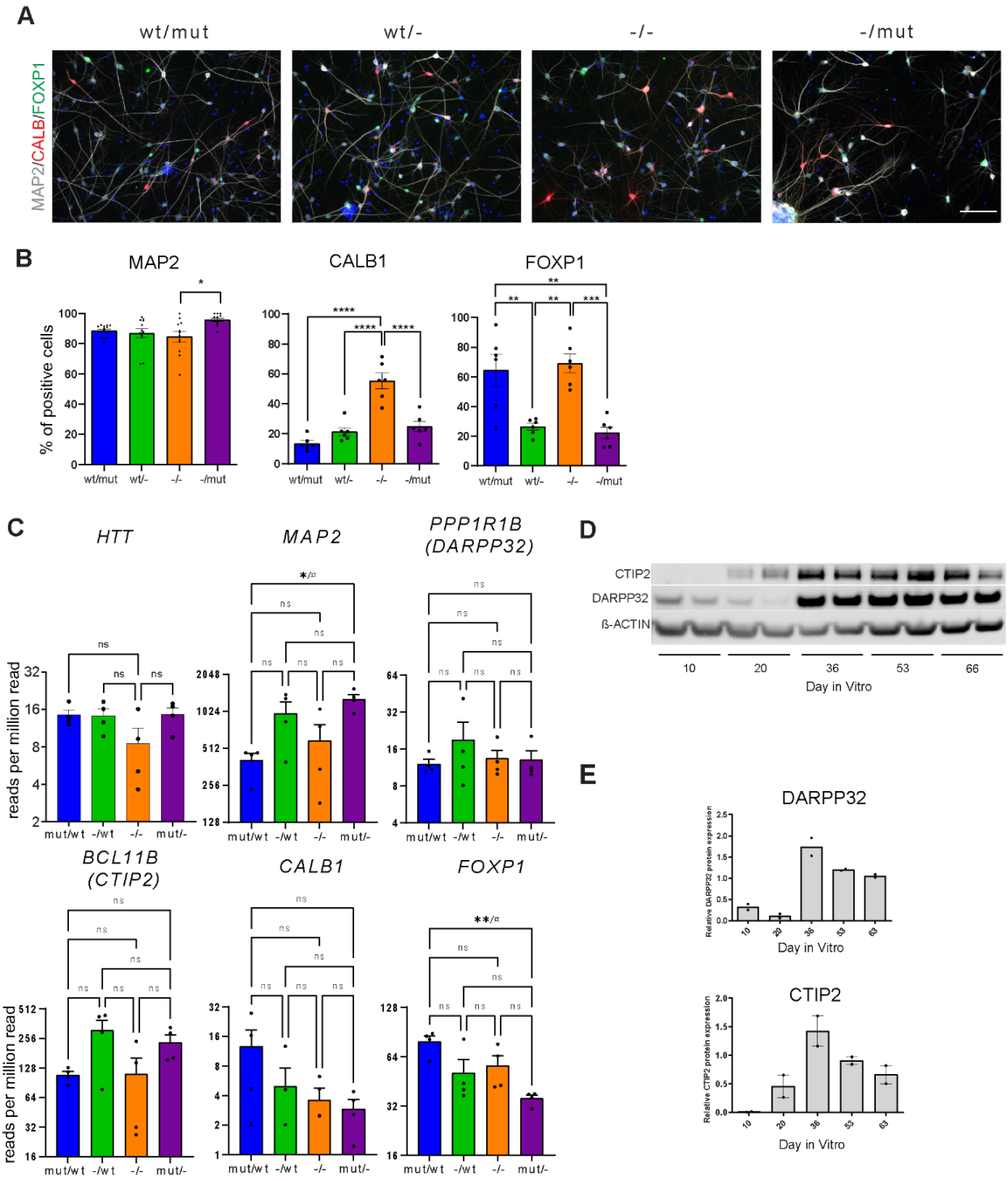

Supplementary Figure 5. Striatal differentiation of isogenic HTTwt/mut, HTTwt/-; HTT-/mut and HTT-/- iPSC cells. All iPS isoclones are able to be differentiate in neurons but the loss of wt-HTT, mut-HTT or both wt and mut-HTT in human iPSC affect the neuronal yield and level of neuronal and SPNs markers. A) Representative immunostaining of neuronal marker (MAP2) and SPNs marker (CALB1 and FOXP1) at DIV55 (scale bar: 100 µm). B) Percentage of cells expressing each marker. Individual data point, mean and SEM are shown (1 clone per genotype,

n=6-12; *p<0.05; **p<0.01; ***p<0.001. C) RNAseq expression data for neuronal gene (MAP2) and genes expressed in SPNs (PPP1R1B (DARPP32); BCL11B (CTIP2), CALB1 and FOXP1) expressed in read per million reads. Individual data point, mean and SEM are shown (n=2 differentiation per clones, n= 2 clones per genotype; one-way ANOVA test with Tukey's multiple comparison post-test; *p <0.05; **p <0.01). D) Representative western blot using two antibodies targeting DARPP32 and CTIP2. E) Quantification of DARPP32 and CTIP2 level during SPNs differentiation at DIV 10 / 20 / 36 / 53 / 66. SPNs were differentiated from hES line RC9 (one experiment, n= 2 / time point, individual data point, mean and SEM are shown).

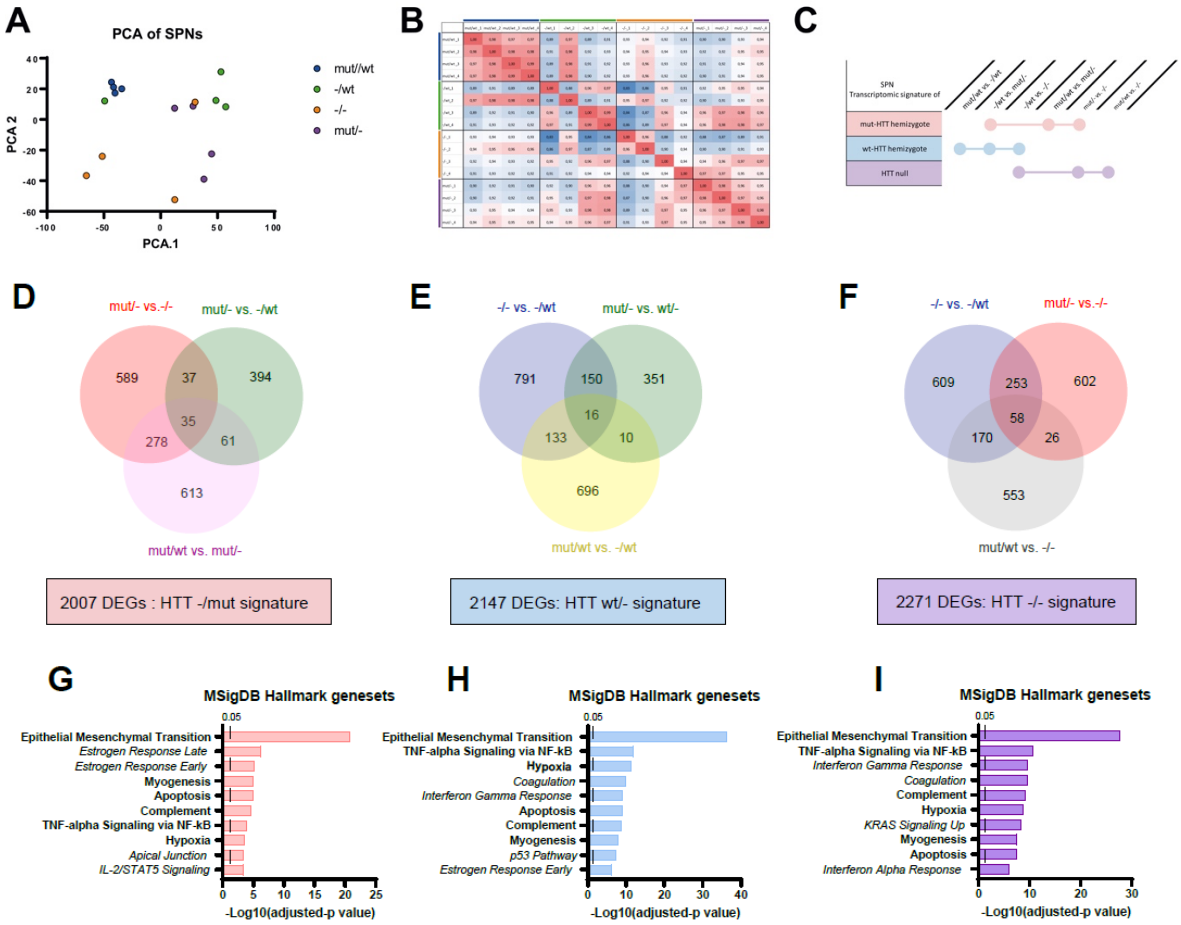

Supplementary Figure 6. Transcriptomes of SPNs derived from isogenic series of the 109Q hiPSC line exhibited different patterns. A) PCA analyses of RNAseq data of isogenic series from the 109Q iPSC line and (B) a correlation matrix of each sample, shows no clustering by genotype of the different isogenic clones (2clones by genotype n=2 per clones). C) Table summarized pairwise comparison of genotype used to defined three transcriptomic signatures (mutant-HTT gain of function; wild-type-HTT gain of function and wild-type and/or mutant-HTT loss of function. D) Venn diagram, KEGG and MSigDB Hallmark gene set enrichment score of the 204 DEGs for the transcriptomic signatures of mut-HTT gain of function. E) Venn diagram, KEGG and MSigDB Hallmark gene set enrichment score of the 484 DEGs for the transcriptomic signatures of wt-HTT loss of function. F) Venn diagram, KEGG and MSigDB Hallmark gene set enrichment score of the 507 DEGs for the transcriptomic signatures of total HTT loss. G-I) Venn diagram of TOP25 MSigDB Hallmark gene set of pairwise comparison by signature.

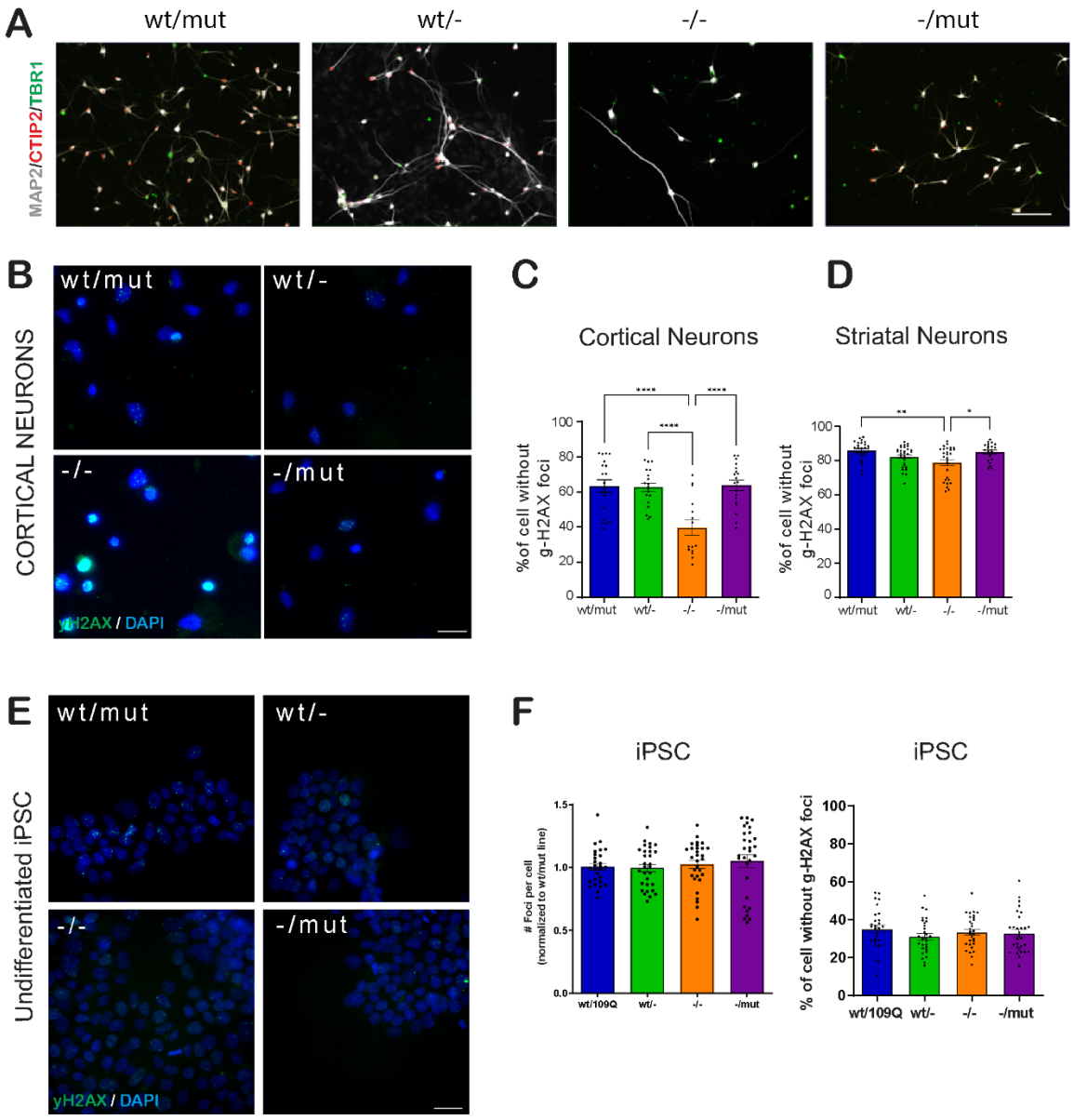

Supplementary Figure 7. Mutation or loss of HTT isoforms impair DNA damage response. A) Representative immunostaining of neuronal marker (MAP2) and cortical marker (CTIP2, TBR1) in cortical neurons at DIV 55 derived from isogenic series of the 109Q hiPSC line (scale bar 100 µm). B) Immunostaining of yH2AX marker (green) to identified double-stranded DNA breaks and DNA staining (DAPI, blue) in Cortical neurons at DIV 55 derived from isogenic series of the 109Q hiPSC line (scale bar 20 µm). C) Percentage of cells (cortical neuron culture) without foci (Individual data points (mean of 20 pictures/well) and median are shown; N indicates the number of neurons per condition in at least two independent experiments; N=11,001 wt/mut; N=11,498 wt/-; N=8,196 -/-; N=11,175 -/mut; ****p<0.0001, one-way ANOVA test with Tukey's multiple comparison post-test). D) Percentage of cells (striatal neuron culture) without foci (Individual data points (mean of 20 pictures/well) and mean and SEM are shown; n indicates the number of neurons per condition in at least four independent experiments; n=31,251 wt/mut; n=33,513 wt/-; n=24,597 -/-; n = 27,809 -/mut; *p<0.05, **p<0.01, ****p<0.0001, one-way ANOVA test with Tukey's

multiple comparison post-test). E) Immunostaining of yH2AX marker (green) to identified double-stranded DNA breaks and DNA staining (DAPI, blue) in iPSC from isogenic series of the 109Q hiPSC line (scale bar 20 μm). F) Number of Foci per cells normalized to HTTwt/mut line and quantification of the percentage of cells without foci (Individual data points (mean of 20 pictures /well) and mean and SEM are shown; N indicates the number of iPSC per condition for 2 clones by genotypes in at least 2 independent experiments; n=7,620 wt/mut; n=6,039 wt/-; n=10,268 -/-; n=8,923 -/mut).

MATERIALS AND METHODS

Flow cytometry

For flow cytometry staining, hiPSC grown in iPSC medium were harvested with trypsin. Briefly, cells were resuspended in PBS-2% FBS and stained with antibodies for 30 minutes at 4°C: Alexa Fluor® 647 anti-human TRA-1-81 Antibody (Biolegend; 330706; 1/50) and PE anti-human/mouse SSEA-3 Antibody (Biolegend; 330312; 1/20). Data were acquired on a Macsquant (MiltenyiBiotec) and analyzed with FlowJo software.

HTT gene editing control by TIDE analysis

Genomic DNA was extracted from iPSCs with the QuickExtract DNA Extraction Solution according to the manufacturer's instruction (Lucigen). We measured gDNA concentration with a Nanodrop spectrophotometer (NanoDrop™ ONE, OZYME, France) and store gDNA as 100 ng/µL solution at -20°C. The PCR amplification was performed on 30 ng of gDNA with the KAPA HiFi Hotstart kit, as previously described [1] with the following primers: HTT-fwd: TTGCTGTGTGAGGCAGAACCTGCGG, and HTT-rev: TGCAGCGGCTCCTCAGCCAC. The resulting PCR products were purified with the gel and PCR clean-up (Machery-Nagel, Düren, Germany), according to the manufacturer's recommendations and eluted in sterile water (Gibco, LifeTechnologies, Zug, Switzerland). PCR product concentration was assessed with a Nanodrop spectrophotometer and each sample was sequenced with the HTT-fwd primer (Microsynth, Balgach, Switzerland). The sequencing chromatograms were analyzed with the Tracking of Indels by Decomposition (TIDE) method [2]. The indel size range was set to 10 or 35 and the size of the decomposition window was adapted for reads of low quality or containing repetitive sequences. The significance cutoff was set to 0.05 (https://tide.nki.nl/).

RNA-Seq library preparation and sequencing

For each sample, 100 ng of total RNA was used to perform the QuantSeq 3' mRNA-Seq Library Prep for Ion Torren (Lexogene) resulting in NGS libraries which originate from the 3' end of polyadenylated RNA. Briefly, library generation was started by oligo(dT) priming with primers already containing the Ion Torrent-specific P1. After first strand synthesis, the RNA was removed before the second strand synthesis was initiated by random primers. Libraries were PCR amplified and barcoded in 13 cycles and were quantified using Agilent High Sensitivity DNA kit (Agilent).

100 pM of 10 libraries were combined, emulsion PCR and enrichment was performed on the Ion OT2 system Instrument using the Ion PI Hi-Q OT2 200 kit (Thermofisher Scientific). Samples were loaded on an Ion PI v3 Chip and sequenced on the Ion Proton System using Ion PI Hi-Q sequencing 200 kit chemistry (200 bp read length; Thermofisher Scientific). Data Analysis: The Ion Proton reads (FASTQ files) were imported into the RNA-seq pipeline of Partek Flow software (v6 Partek Inc) using hg19 as a reference genome and Refseq 2019. To determine genes that are differentially expressed between groups mapped reads were quantified using Partek E/M algorithm normalised by the Total count/sample (the resulting counts represent the gene expression levels on reads/millions for over 20,800 different genes present in the AmpliSeq Human Gene Expression panel. Differentially expressed genes were identified using Partek Gene Specific Analysis (GSA) algorithm.

To investigate the transcriptional changes mediated by loss of wt-, mut- or both wt/mut-HTT in undifferentiated human iPSCs, we performed genome-wide RNA sequencing on 3 to 4 clones of each genotype and on four independent cultures of the parental 109Q-iPSC line. Principal component analysis revealed that transcriptional profiles separated poorly according to genotypes (Fig. 1E). Differentially expressed genes (DEG) were identified by pairwise comparison across all genotypes (adjusted p-value ≤ 0.05; Fold change ≥ 1.25). We then joint by three, the DEG lists of pairwise comparisons sharing the same reference samples to generate three "combined" lists of gene differentially expressed in HTT-/mut (2,259 genes), HTTwt/- (1,532 genes) or HTT-/- (1377 genes) iPSCs when compared to iPSCs from any of other genotypes (Supplementary Figure 3A-E). Gene set enrichment analysis of these combined lists demonstrated their significant enrichment in several MSigDB Hallmark genesets (Supplementary Figure 3F-H) [3]. Surprisingly, the top 10 of most enriched genesets for each combined list included more than half (6/10) genesets enriched in all three lists. All six pathways, mTORC1, Oxidative phosphorylation, Cholesterol Homeostasis, DNA repair, glycolysis, and Fatty acid metabolism have already been linked to HD pathology in animal model or patients [4–8]. Their alterations in HD might thus be triggered by a loss of HTT protein and could occurs already in pluripotent cells in human HD embryos.

To investigate the transcriptional change mediated by the loss of wt-, mut-, or wt/mut-HTT in striatal neurons, we performed genome-wide RNA sequencing of DIV55 striatal cultures from two clones of each genotype each differentiated twice independently. Differential gene expression was assessed pairwise across all genotypes (adjusted p-value ≤ 0.05; Fold change ≥ 1.25) and we

generated differentially expressed genes (DEGs) lists and combined lists as described for iPSC with the same three categories (Supplementary Figure 3B and 6C). The number of DEGs in the three combined lists ranged from 2,007 genes for the HTT-/mut SPNs signature to 2,271 genes for the HTT-/- SPNs signature (Supplementary Figure 6D-F). Gene set enrichment analysis of the three combined DEG lists for SPN samples demonstrated their significant enrichment in several MSigDB Hallmark genesets (Supplementary Figure 6D-F). The top 10 of most enriched genesets for each combined list (Supplementary Figure 6G-I) included again more than half of the genesets enriched in all three lists (6/10: epithelial mesenchymal transition, TNF-alpha signaling via NF-KB, Hypoxia, Apoptosis, Complement, Myogenesis (Supplementary Figure 6G-I). Among these six pathways, epithelial mesenchymal transition, Hypoxia, Apoptosis, were significantly enriched (adjusted p-value <0.05) in at least one combined DEG lists from the iPS sample RNAseq. Likewise, the three genesets: cholesterol homeostasis, mTORC1 signaling and glycolysis we found enriched in all iPS DEG lists were as well significantly enriched in up to 3/3 of the SPN DEG lists. These results suggest that the alterations of these last 6 pathways which have all already been linked to HD [5,6,8–11] might involve an HTT loss of function component and could occurs throughout neuronal development and not just in adult brain cells.

Neural differentiation

For neural differentiation, hiPSC colonies were treated (DIV0) as previously described [12] in N2B27 media consisting of 50% DMEMF-12 Glutamax, 50% Neurobasal medium, 2% B27 supplement 50× minus vitamin A, 1% N2 supplement and 50 μM β-mercaptoethanol (Thermo Fisher Scientific). Neural differentiation was initiated, passaging the hiPSC in N2B27 media supplemented with SB431542 (20 μM; Tocris), LDN-193189 (100 nM; Sigma-Aldrich), XAV-939 (1 μM; Tocris), and 10 μM ROCK inhibitor (Y27632, Calbiochem) in low-adherence culture plate (Greiner) for 6 h. Media were changed every day from DIV0 to DIV6. At DIV1, hiPSC aggregates were transferred on poly-ornithine (Sigma) laminin (Thermo Fisher Scientific)-coated dishes without Y27632. From DIV3 to DIV6, FGF2 (10 ng/ml) was added. At DIV5 SB431542 was removed. For spindle orientation and mitotic index experiment cells were fixed at DIV 7.

Striatal projecting neurons differentiation

For striatal projecting neurons (SPNs) differentiation, hiPSC or hESC colonies were treated (DIV0) as previously described in [12,13] in N2B27 media consisting of 50% DMEMF-12 Glutamax, 50% Neurobasal medium, 2% B27 supplement 50× minus vitamin A, 1% N2 supplement, 0.1% penicillin/streptomycin, and 50 μM β-mercaptoethanol (Thermo Fisher Scientific). Neural differentiation was initiated, passaging the hiPSC or hESC in N2B27 media supplemented with SB431542 (20 μM; Tocris), LDN-193189 (100 nM; Sigma-Aldrich), XAV-939 (1 μM; Tocris), and 10 μM ROCK inhibitor (Y27632, Calbiochem) in low-adherence culture plate (Greiner) for 6 hours. Then hiPSC aggregates were transferred on poly-ornithine (Sigma) laminin (Thermo Fisher Scientific)-coated dishes. Media were changed every day from DIV0 to DIV20. Y27632 and SB431542 were removed respectively at DIV 1 and DIV 5.

At DIV10, Splitting was done using EDTA onto poly-ornithine (Sigma) laminin (Thermo Fisher Scientific)-coated dishes at a ratio of 1:1. From DIV10 to DIV20, LDN-193189 was removed and Activin A (50 ng/ml; Peprotech) was added. At DIV20, SPNs precursor cells were enzymatically dissociated using Accutase (Invitrogen), resuspended at 5 × 106 cells/ml in Cryostor (StemCell technology) cell cryopreservation media, frozen, and stored in liquid nitrogen vapor at −150°C.

SPNs precursors were suspended in N2B27 medium supplemented with BDNF (20 ng/ml; PeproTech), cAMP (100 μM; Merck), Activin A (50 ng/ml; Peprotech) and ROCK inhibitor (Y-27632; STEMCELL Technologies) and plated on poly-ornithine (Sigma) laminin (Thermo Fisher Scientific)-coated dishes to a final density of ~100 000 cells/cm^2. Y-27632 was remove the next day with a complete medium change, and then half of the medium was change once a week.

Cortical differentiation

For cortical neurons differentiation, hiPSC colonies were treated (DIV0) as previously described [14] in N2B27 media consisting of 50% DMEMF-12 Glutamax, 50% Neurobasal medium, 2% B27 supplement 50× minus vitamin A, 1% N2 supplement, 0.1% penicillin/streptomycin, and 50 μM β-mercaptoethanol (Thermo Fisher Scientific). Neural differentiation was initiated, passaging the hiPSC in N2B27 media supplemented with SB431542 (20 μM; Tocris), LDN-193189 (100 nM; Sigma-Aldrich), XAV-939 (1 μM; Tocris), and 10 μM ROCK inhibitor (Y27632, Calbiochem) in low-adherence culture plate (Greiner) for 6 h. Then

hiPSC aggregates were transferred on poly-ornithine (Sigma) laminin (Thermo Fisher Scientific)-coated dishes. Media were changed every day from DIV0 to DIV20. At DIV1, Y27632 was removed. From DIV5 to DIV9, SB431542 was removed and FGF2 (10 ng/ml) and cyclopamine 1 μM (Merck) were added.

At DIV10, Splitting was done adding EDTA onto poly-ornithine (Sigma) laminin (Thermo Fisher Scientific)-coated dishes at a ratio of 1:1. From DIV10 to DIV20, LDN-193189 and XAV-939 were removed and CHIR99021 0.4 μM (Stemgent) was added. At DIV20, cortical neuron precursor cells were enzymatically dissociated using Accutase (Invitrogen), resuspended at 5 × 106 cells/ml in Cryostor (Merck) cell cryopreservation media, frozen, and stored in liquid nitrogen vapor at −150°C.

Cortical neuron precursors were suspended in N2B27 medium supplemented with BDNF (20 ng/ml; PeproTech), cAMP (100 μM; Merck), DAPT (10 μM; Tocris) and ROCK inhibitor (Y-27632; STEMCELL Technologies) and plated on poly-ornithine (Sigma) laminin (Thermo Fisher Scientific)-coated dishes to a final density of ~100,000 cells/cm2. Y-27632 was remove the next day with a complete medium change, and then half of the medium was changed once a week. After the first week; DAPT concentration was decrease to 5 μM and one week later to 1 μM.

Protein extraction and western blotting

In order to extract cell protein and perform western blot analysis cells were lyzed in RIPA 1× buffer (Sigma®) containing protease inhibitors (Sigma®) and phosphatase inhibitors (Roche®). Proteins were quantified by Pierce BCA Protein Assay kit (Pierce®). Protein extracts (5-10 μg) were loaded on a 3–8% (NuPage Tris-Acetate gels, Invitrogen®) or 10% (NuPage Bis–Tris gels, Invitrogen®) and transferred onto Gel Transfer Stacks Nitrocellulose membranes (Invitrogen®) using the iBlot2 Dry Blotting System (Invitrogen®). Membranes were then incubated overnight at 4°C with the following primary antibodies diluted in PBS-BSA-Triton buffer [phosphate buffered saline (PBS, Sigma #P4417) supplemented with 5% bovine serum albumin (BSA, Sigma #A7906) and 0.01% Tween 20 (Prolabo , 28829-296): CTIP2 (Abcam; ab18465; 1/1000); D7F7 (Cell signaling; 5656; 1/1000); DARPP32 (Abcam; ab40801; 1/500); MAP2 (Biolegend; 822501; 1/10000); OCT4 (Cell Signaling; 28405; 1/600); P1874 (Merck Sigma-Aldrich; p1874; 1/1000); PAX6 (Biolegend; 901301; 1/1000); β-ACTIN (Merck Sigma-Aldrich; A3854; 1/50000).

Membranes were washed 3 times with PBS-T [PBS supplemented with 0.1% Tween 20] (for 10 minutes each time) and incubated with secondary antibodies diluted in PBS-T-BSA: donkey anti-rabbit 800CW IRDye® (1:15000, Li-Cor #926-32213),donkey anti-mouse 680RD IRDye® (1:15000, Li-Cor #926- 68072), donkey anti-chicken 800RD IRDye® (1:15000, Li-Cor #926-32218) during 1 h at RT. Membranes were washed 3 times in PBS-T before quantification of antibody binding using a LiCor Odyssee CLx machine and Image Studio Lite 5.2 software. For Fig. 1C, Individual data points and median are shown as fold change compared to HTTwt/mut cells, n=4/genotype. *p < 0.05, **p <0.01, one-way ANOVA test with Tukey's multiple comparison post-test. For Fig. 3C, Protein level (Band intensities) were quantified and normalized to the level of β-Actin housekeeping protein and to the median of levels recorded for HTTwt/mut samples. Individual data points and median are shown, (n=3 independent maturation of 2 independent differentiation per clones; 1-2 clones per genotype; *p <0.05, ****p<0.0001, one-way ANOVA test with Tukey's multiple comparison post-test). For Fig. 3E, Band intensities were quantified and values normalized to the Actin housekeeping protein. Individual data points and median are shown, n=3 - 9 per hPSC lines. *p <0.05, ****p<0.0001, one-way ANOVA test with Tukey's multiple comparison post-test.

Spindle orientation quantification and image analyses

Spindle angle in metaphase cells stained for pericentrin and DAPI to visualize the spindle poles, the lumen outer limit and chromatin was calculated using ImageJ software (http://rsb.info.nih.gov/ij/, NIH, USA). The images were capture with a Leica DMI6000 confocal optical microscope (TCS SPE) equipped with a 63x oil-immersion objective controlled by LAS X software. Z-stack steps were of 0.64 µm. For hiPSC, the angle between the pole-pole axis and the substratum plane was calculated. A line crossing both spindle poles was drawn on the Z projection pictures and repositioned along the Z-axis using the stack of Z-sections. For R-NSC, one line crossing both spindle poles and the tangent of the lumen outer limit were drawn on the Z projection pictures to determine the angle.

BDNF transport

Cortical progenitors were suspended in N2B27 medium (50% DMEMF-12 Glutamax, 50% Neurobasal medium, 2% B27 supplement 50x minus vitamin A, 1% N2 supplement and 50 µM β-

mercaptoethanol from ThermoFisher) and plated to a final density of 100,000 cells/well, previously coated with poly-D-lysine/laminin in the distal compartment. For the final differentiation cells were cultivated in N2B27 medium supplemented with BDNF (20 ng/ml, Peprotech), cAMP (100 µM, Merck), DAPT (10µM, Tocris), Cdk4i (1µM, Merck), and rock inhibitor (Y-27632, 10 µM, Stemcell technologies). Before plating, neurons in suspension, were infected with BDNF-mCherry lentivirus during 1 h. The day after infection and every 7 days, the medium were replaced by fresh N2B27 supplemented medium without rock inhibitor. At DIV17, we used an inverted microscope (Axio Observer, Zeiss) coupled to a spinning-disk confocal system (CSU-W1-T3, Yokogawa) connected to wide field electron-multiplying CCD camera (ProEM+1024, Princeton Instrument) and maintained at 37°C and 5% CO2. We took images every 200 ms for 30 s BDNF-mCherry trafficking (×63 oil-immersion objective, 1.46 NA). Images were analyzed with the KymoToolBox plugin for ImageJ [15–17]. For Fig. 4E-H, the number of axons per condition in at least three independent experiments is n=49 wt/mut; n =65 wt/-; n=50 -/-; n =61 -/mut; *p <0.05, **p<0.01, ***p<0.001, one-way ANOVA test with Tukey's multiple comparison post-test.).

REFERENCES

[1] Merienne N, Vachey G, de Longprez L, Meunier C, Zimmer V, Perriard G, et al. The self-inactivating KamiCas9 system for the editing of CNS disease genes. Cell Rep. 2017;20:2980–91. https://doi.org/10.1016/j.celrep.2017.08.075.

[2] Brinkman EK, Chen T, Amendola M, van Steensel B. Easy quantitative assessment of genome editing by sequence trace decomposition. Nucleic Acids Res. 2014;42:e168. https://doi.org/10.1093/nar/gku936.

[3] Liberzon A, Birger C, Thorvaldsdóttir H, Ghandi M, Mesirov JP, Tamayo P. The Molecular Signatures Database (MSigDB) hallmark gene set collection. Cell Syst. 2015;1:417–25. https://doi.org/10.1016/j.cels.2015.12.004.

[4] Bettencourt C, Hensman-Moss D, Flower M, Wiethoff S, Brice A, Goizet C, et al. DNA repair pathways underlie a common genetic mechanism modulating onset in polyglutamine diseases. Ann Neurol. 2016;79:983–90. https://doi.org/10.1002/ana.24656.

[5] Block RC, Dorsey ER, Beck CA, Brenna JT, Shoulson I. Altered cholesterol and fatty acid metabolism in Huntington disease. J Clin Lipidol. 2010;4:17–23. https://doi.org/10.1016/j.jacl.2009.11.003.

[6] Dubinsky JM. Towards an understanding of energy impairment in Huntington's disease brain. J Huntingtons Dis. 2017;6:267–302. https://doi.org/10.3233/JHD-170264.

[7] Genetic Modifiers of Huntington's Disease (GeM-HD) Consortium. Identification of genetic factors that modify clinical onset of Huntington's disease. Cell. 2015;162:516–26. https://doi.org/10.1016/j.cell.2015.07.003.

[8] Pryor WM, Biagioli M, Shahani N, Swarnkar S, Huang W-C, Page DT, et al. Huntingtin promotes mTORC1 signaling in the pathogenesis of Huntington's disease. Sci Signal. 2014;7:ra103. https://doi.org/10.1126/scisignal.2005633.

[9] Burtscher J, Maglione V, Di Pardo A, Millet GP, Schwarzer C, Zangrandi L. A rationale for hypoxic and chemical conditioning in Huntington's disease. Int J Mol Sci. 2021;22:582. https://doi.org/10.3390/ijms22020582.

[10] Hickey MA, Chesselet MF. Apoptosis in Huntington's disease. Prog Neuropsychopharmacol Biol Psychiatry. 2003;27:255–65. https://doi.org/10.1016/S0278-5846(03)00021-6.

[11] Moreira Sousa C, McGuire JR, Thion MS, Gentien D, de la Grange P, Tezenas du Montcel S, et al. The Huntington disease protein accelerates breast tumour development and metastasis through ErbB2/HER2 signalling. EMBO Mol Med. 2013;5:309–25. https://doi.org/10.1002/emmm.201201546.

[12] Nicoleau C, Varela C, Bonnefond C, Maury Y, Bugi A, Aubry L, et al. Embryonic stem cells neural differentiation qualifies the role of Wnt/beta-catenin signals in human telencephalic specification and regionalization. Stem Cells. 2013;31:1763–74. https://doi.org/10.1002/stem.1462.

[13] Arber C, Precious SV, Cambray S, Risner-Janiczek JR, Kelly C, Noakes Z, et al. Activin A directs striatal projection neuron differentiation of human pluripotent stem cells. Development. 2015;142:1375–86. https://doi.org/10.1242/dev.117093.

[14] Gribaudo S, Bousset L, Courte J, Melki R, Peyrin J-M, Perrier AL. Propagation of distinct alpha-synuclein strains within human reconstructed neuronal network and associated

neuronal dysfunctions. Protein Aggregation. Recent Developments in Structural Studies of Protein Fibrillation and Coacervation Within and Without Cellular Context, 2022.

[15] Zala D, Hinckelmann M-V, Yu H, Lyra da Cunha MM, Liot G, Cordelières FP, et al. Vesicular glycolysis provides on-board energy for fast axonal transport. Cell. 2013;152:479–91. https://doi.org/10.1016/j.cell.2012.12.029.

[16] Gauthier LR, Charrin BC, Borrell-Pages M, Dompierre JP, Rangone H, Cordelieres FP, et al. Huntingtin controls neurotrophic support and survival of neurons by enhancing BDNF vesicular transport along microtubules. Cell. 2004;118:127–38.

[17] Virlogeux A, Moutaux E, Christaller W, Genoux A, Bruyère J, Fino E, et al. Reconstituting corticostriatal network on-a-chip reveals the contribution of the presynaptic compartment to Huntington's disease. Cell Rep. 2018;22:110–22. https://doi.org/10.1016/j.celrep.2017.12.013.